Int. J. Electrochem. Sci., 8 **(2013)** 11474 - 11491

International Journal of
ELECTROCHEMICAL
SCIENCE
www.electrochemsci.org

An Experimental and Theoretical Investigation of Adsorption Characteristics of a Quinoxaline Compound as Corrosion Inhibitor at Carbon Steel/Hydrochloric Acid Interface

H. Zarrok[1], *A. Zarrouk*[2,*], *R. Salghi*[3], *B. Elmahi*[2], *B. Hammouti*[2], *S. S. Al-Deyab*[4], *M. Ebn Touhami*[5], *M. Bouachrine*[6], *H. Oudda*[1], *S. Boukhris*[7]

[1] Laboratoire des procèdes de séparation, Faculté des Sciences, Université Ibn Tofail, Kénitra, Morocco.
[2] LCAE-URAC18, Faculté des Sciences, Université Mohammed 1er, Oujda, Morocco.
[3] Equipe de Génie de l'Environnement et Biotechnologie, ENSA, Université Ibn Zohr, BP1136 Agadir, Morocco.
[4] Petrochemical Research Chair, Chemistry Department, College of Science, King Saud University, P.O. Box 2455, Riyadh 11451, Saudi Arabia.
[5] Laboratoire d'électrochimie, de corrosion et d'environnement, Faculté des Sciences, Université Ibn Tofail BP 242, 14000 Kenitra, Morocco.
[6] ESTM, Université Moualy Ismail, Meknes, Morocco.
[7] Laboratoire de Synthèse Organique, Organométallique et Théorique, Faculté des Sciences, Université Ibn Tofail, B.P. 133, 14000 Kenitra, Morocco.
[*]E-mail: azarrouk@gmail.com

Received: 13 April 2013 / *Accepted:* 7 August 2013 / *Published:* 20 August 2013

This study investigates the effect of a quinoxaline namely ethyl 2-(4-(2-ethoxy-2-oxoethyl)-2-*p*-tolylquinoxalin-1(4*H*)-yl) acetate (Q3), on corrosion inhibition of carbon steel in 1.0 M HCl. Electrochemical impedance measurement, potentiodynamic polarization and weight loss methods were applied to study adsorption of Q3 at metal/solution interface. Some quantum chemical parameters and the optimized structure of Q3 were calculated using the B3LYP/6-31G (d,p) basis. Results revealed that Q3 is an excellent inhibitor for carbon steel corrosion in 1.0 M HCl; showing a maximum efficiency 97.4% at concentration of 10^{-3}M. Values of inhibition efficiency obtained from weight loss, potentiodynamic polarization, and electrochemical impedance spectroscopy (EIS) are in good agreement. Polarization curves show that Q3 behaves as a mixed-type inhibitor in hydrochloric acid. EIS shows that charge-transfer resistance increase and the capacitance of double layer decreases with the inhibitor concentration, confirming the adsorption process mechanism. Its was shown that adsorption is consistent with the Langmuir isotherm for 308K. The negative free energy of adsorption in the presence of Q3 suggests chemisorption of quinoxaline molecules on the steel surface. Results obtained from theoretical study were found to confirm experimental findings.

Keywords: Quinoxaline, Steel, Corrosion inhibition, Electrochemical techniques, DFT.

1. INTRODUCTION

The use of inhibitors to control the destructive attack of acid environment has found widespread applications in many industrial processes such as acid cleaning, acid pickling, acid descaling, and oil well acidizing [1]. The applicability of organic compounds as corrosion inhibitors for metals in acidic media has been recognized for a long time [2-4]. Most of the effective organic inhibitors used contain heteroatoms such as O, N, S and multiple bonds in their molecules through which they are adsorbed on the metal surface [5-23]. It has been observed that adsorption depends mainly on certain physico-chemical properties of the inhibitor group, such as functional groups, electron density at the donor atom, π-orbital character, and the electronic structure of the molecule [24].

Hydrochloric acid (HCl) is widely used in the acid pickling of steel and ferrous alloys, acid cleaning, acid rescaling, oil well cleaning, petrochemical industry and various electrochemical systems. Hence, much attention is needed on corrosion inhibitors to reduce the corrosion rates of metallic materials.

In the present work, a systematic study has been undertaken to understand the corrosion behaviour of carbon steel and the inhibitive action of ethyl 2-(4-(2-ethoxy-2-oxoethyl)-2-*p*-tolylquinoxalin-1(4*H*)-yl) acetate (Q3) in 1.0 M HCl environment, using weight loss, Tafel polarization, and impedance techniques; the effect of the molecular structure on the chemical reactivity has been object of great interest in several disciplines of chemistry. In this respect, quantum chemical calculations have been widely used to investigate the molecule in its electronic structure level and to interpret the experimental results. The inhibition property of a compound has been often correlated with molecular properties. The chemical structure of the studied quinoxaline derivative is given in Figure 1.

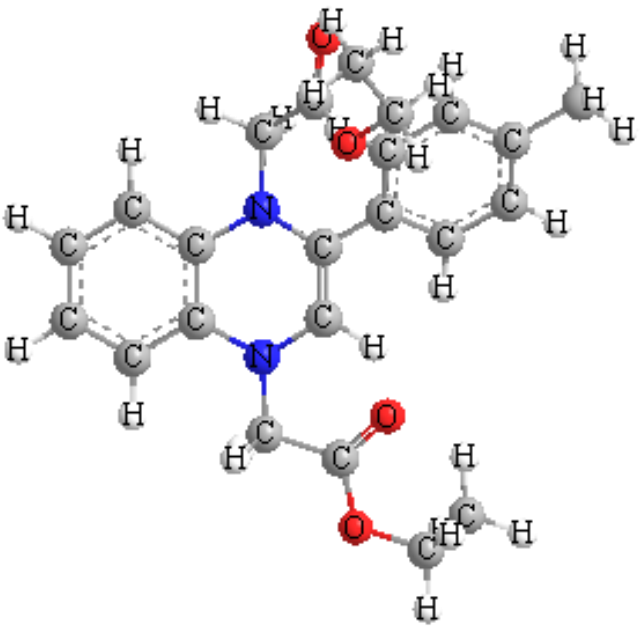

Figure 1. The chemical structure of the studied quinoxaline compound.

2. EXPERIMENTAL METHODS

2.1. Materials

The steel used in this study is a carbon steel (Euronorm: C35E carbon steel and US specification: SAE 1035) with a chemical composition (in wt%) of 0.370 % C, 0.230 % Si, 0.680 % Mn, 0.016 % S, 0.077 % Cr, 0.011 % Ti, 0.059 % Ni, 0.009 % Co, 0.160 % Cu and the remainder iron (Fe). The carbon steel samples were pre-treated prior to the experiments by grinding with emery paper SiC (120, 600 and 1200); rinsed with distilled water, degreased in acetone in an ultrasonic bath immersion for 5 min, washed again with bidistilled water and then dried at room temperature before use. The acid solutions (1.0 M HCl) were prepared by dilution of an analytical reagent grade 37 % HCl with double-distilled water. The concentration range of Q3 employed was 10^{-6} M to 10^{-3} M.

2.2. Measurements

2.2.1. Weight loss measurements

The steel sheets of 1.6 × 1.6 × 0.07 cm dimensions were abraded with different grades of emery papers, washed with distilled water, degreased with acetone, dried and kept in a desiccator. After weighing accurately by a digital balance with high sensitivity the specimens were immersed in solution containing 1.0 M HCl solution with and without various concentrations of the investigated inhibitor. At the end of the tests, the specimens were taken out, washed carefully in ethanol under ultrasound until the corrosion products on the surface of carbon steel specimens were removed thoroughly, and then dried, weighed accurately. Duplicate experiments were performed in each case and the mean value of the weight loss is reported. Weight loss allowed calculation of the mean corrosion rate in mg cm^{-2} h^{-1}. The corrosion rate (ν) and the inhibition efficiency (η_{WL}) were calculated by the following equations:

$$\nu = \frac{W}{St} \times 100 \quad (1)$$

$$\eta_{WL}(\%) = \frac{\nu_0 - \nu}{\nu_0} \times 100 \quad (2)$$

where W is the three-experiment average weight loss of the carbon steel, S is the total surface area of the specimen, t is the immersion time and ν_0 and ν are values of the corrosion rate without and with addition of the inhibitor, respectively.

2.2.2. Electrochemical measurements

❖ *Electrochemical impedance spectroscopy*

The electrochemical measurements were carried out using Volta lab (Tacussel- Radiometer PGZ 100) potentiostate and controlled by Tacussel corrosion analysis software model (Voltamaster 4) at under static condition. The corrosion cell used had three electrodes. The reference electrode was a

saturated calomel electrode (SCE). A platinum electrode was used as auxiliary electrode of surface area of 0.094 cm^2. The working electrode was carbon steel. All potentials given in this study were referred to this reference electrode. The working electrode was immersed in test solution for 30 minutes to a establish steady state open circuit potential (*E*ocp). After measuring the *E*ocp, the electrochemical measurements were performed. All electrochemical tests have been performed in aerated solutions at 308 K. The EIS experiments were conducted in the frequency range with high limit of 100 kHz and different low limit 0.1 Hz at open circuit potential, with 10 points per decade, at the rest potential, after 30 min of acid immersion, by applying 10 mV ac voltage peak-to-peak. Nyquist plots were made from these experiments. The best semicircle can be fit through the data points in the Nyquist plot using a non-linear least square fit so as to give the intersections with the *x*-axis.

The inhibition efficiency of the inhibitor was calculated from the charge transfer resistance values using the following equation [25]:

$$\eta_z\% = \frac{R_{ct(inh)} - R_{ct}}{R_{ct(inh)}} \times 100 \quad (1)$$

where R_{ct} and $R_{ct(inh)}$ were the values of polarization resistance in the absence and presence of inhibitor, respectively.

❖ *Potentiodynamic polarization*

The electrochemical behaviour of carbon steel sample in inhibited and uninhibited solution was studied by recording anodic and cathodic potentiodynamic polarization curves. Measurements were performed in the 1.0 M HCl solution containing different concentrations of the tested inhibitor by changing the electrode potential automatically from -800 to 0 mV versus corrosion potential at a scan rate of 1 mV s^{-1}. The linear Tafel segments of anodic and cathodic curves were extrapolated to corrosion potential to obtain corrosion current densities (I_{corr}). From the polarization curves obtained, the corrosion current (I_{corr}) was calculated by curve fitting using the equation:

$$I = I_{corr}\left[exp\left(\frac{2.3\Delta E}{\beta_a}\right) - exp\left(\frac{2.3\Delta E}{\beta_c}\right)\right] \quad (2)$$

The inhibition efficiency was evaluated from the measured I_{corr} values using the relationship:

$$\eta_{Tafel}\% = \frac{I^{\circ}_{corr} - I^{i}_{corr}}{I^{\circ}_{corr}} \times 100 \quad (3)$$

where, I°_{corr} and I^{i}_{corr} are the corrosion current density in absence and presence of inhibitor, respectively.

2.2.3. Quantum chemical calculations

All theoretical calculations were performed using DFT (density functional theory) with the Beck's three parameter exchange functional along with the Lee-Yang-Parr nonlocal correlation functional (B3LYP) [26-28] with 6- 31G* basis set is implemented in Gaussian 03 program package [29]. This approach is shown to yield favorable geometries for a wide variety of systems. The following quantum chemical parameters were calculated from the obtained optimized molecular structure: the energy of the highest occupied molecular orbital (E_{HOMO}), the energy of the lowest unoccupied molecular orbital (E_{LUMO}), the energy band gap ($\Delta E_{gap} = E_{HOMO} - E_{LUMO}$), the dipole moment ($\mu$), the electron affinity (A), the ionization potential (I), the fraction of electrons transferred (ΔN) and softness were calculated and discussed.

3. RESULTS AND DISCUSSION

3.1. Polarization curves

Polarization curves were obtained for carbon steel in 1.0 M HCl solution with and without inhibitor. The polarization exhibits Tafel behavior. Tafel lines which obtained in various concentrations of Q3 in 1.0 M HCl solutions were shown in Fig. 2, at 308K respectively. The corresponding electrochemical parameters, i.e., corrosion potential (E_{corr} versus SCE), corrosion current density (I_{corr}), cathodic and aTafel slopes (β_c) values were calculated from these curves and are given in Table 1.

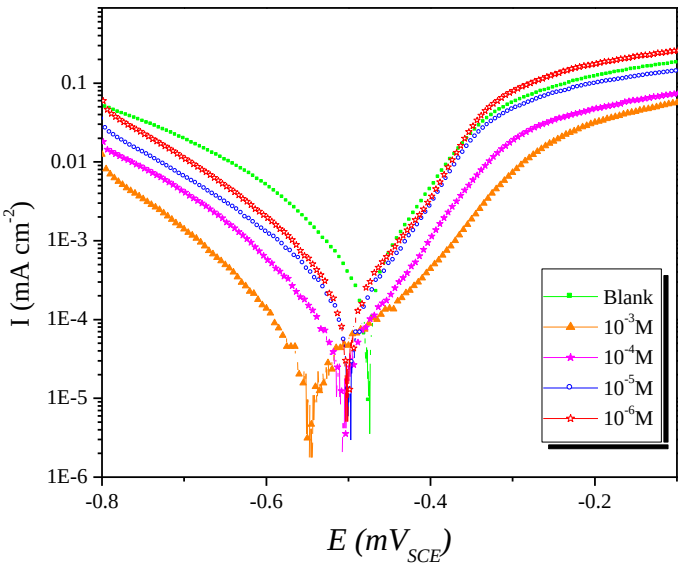

Figure 2. Polarisation curves of carbon steel in 1.0 M HCl for various concentrations of Q3.

The presence of Q3 both anodic and cathodic branches to the lower values of current densities and thus causes a remarkable decrease in the corrosion rate. It can be clearly seen from Fig. 2 that both

anodic metal dissolution of iron and cathodic hydrogen and oxygen evolution reactions were inhibited after the addition of quinoxaline derivative to the aggressive solution. This result is indicative of the adsorption of inhibitor molecules on the active sites of carbon steel surface [30]. The inhibition of both anodic and cathodic reactions is more pronounced with the increasing inhibitor concentration. However, the influence is more pronounced in the cathodic polarization plots compared to that of the anodic polarization plots. The cathodic current-potential curves (Fig. 2) giving rise to parallel lines indicates that the addition of Q3 to the 1.0 M HCl solution does not modify the reduction mechanism and the reduction at carbon steel surface takes place mainly through a charge transfer mechanism [31-33] The slopes do not display an order with the inhibitor concentration; this feature indicates that inhibition occurred by a blocking mechanism on the available metal spaces [34-36]. The corrosion potential displayed small change and curves changed slightly towards the negative direction (Fig. 2). These results indicated that the presence of Q3 compound inhibited iron oxidation and in a lower extent hydrogen and oxygen evolution, consequently these compounds can be classified as mixed corrosion inhibitor, as electrode potential displacement is lower than 85 mV in any direction [37].

Table 1. Polarization data of carbon steel in 1.0 M HCl without and with addition of inhibitor at 308 K.

Inhibitor	Conc (M)	$-E_{corr}$ (mV/SCE)	$-\beta_c$ (mV dec^{-1})	I_{corr} (μA cm^{-2})	η_{Tafel} (%)
Blank	1.0	475.9	176.0	1077.8	-
Q3	10^{-3}	547.4	155.7	54.5	94.9
	10^{-4}	508.0	165.8	109.5	89.8
	10^{-5}	503.1	164.3	230.3	78.6
	10^{-6}	500.0	164.4	362.1	66.4

3.2. Electrochemical impedance spectroscopy

The inhibition efficiencies of Q3 on carbon steel were examined by electrochemical impedance spectroscopy. The impedance spectra of carbon steel in 1.0 M HCl solution in the absence and presence of five different concentrations of quinoxaline derivative were recorded. Fig. 3 shows the impedance spectra in Nyquist format.

The impedance diagrams display one single capacitive loop represented by slightly depressed semi-circle for this compound. This capacitive loop indicates that the corrosion of carbon steel in 1.0 M HCl solution is mainly controlled by charge transfer process and formation of a protective layer on the metal surface. Deviations from the ideal semi-circle are generally attributed to the frequency dispersion as well as inhomogeneities, roughness of metal surface and mass transport process [38-40]. The impedance response of carbon steel in HCl changes with the addition of Q3 into the test solutions and this change more pronounced with increasing inhibitor concentration. The diameter of the capacitive loop increases as the concentration of inhibitor rises, this increase indicates adsorption of inhibitor molecules on the metal surface [41]. On the other hand, the similar nature of impedance

diagrams obtained in the absence and presence of quinoxalines reveal that the addition of inhibitors does not change the mechanism for the dissolution of iron in HCl [42-45].

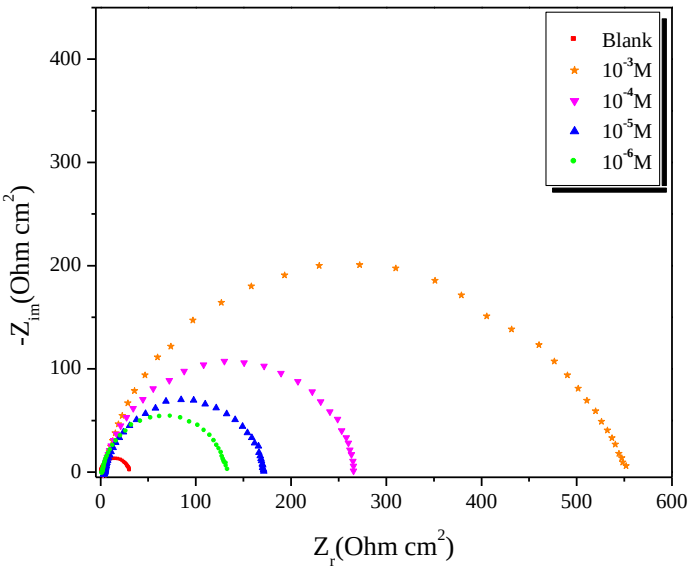

Figure 3. Nyquist plots of carbon steel in 1.0 M HCl solution containing different concentrations of Q3.

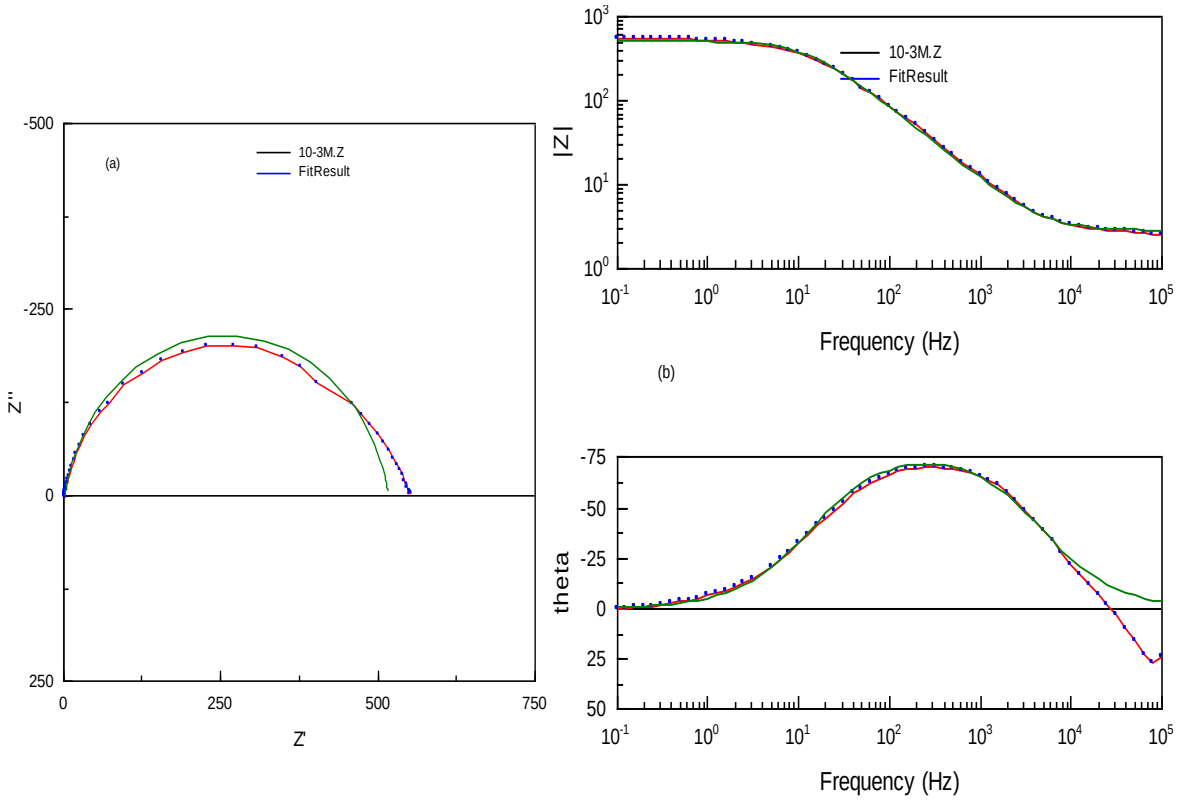

Figure 4. EIS Nyquist (a) and Bode (b) plots for carbon steel/1.0 M HCl + 10^{-3}M Q3 interface: dotted lines experimental data; dashed line calculated.

All experimental spectra were fitted with an appropriate equivalent circuit to find the parameters, which describe and being consistent with the experimental data. Simulation of bode plot with above model shows excellent agreement with experimental data (Fig. 4, representative example).

Fig. 5 depicts the proposed equivalent circuit, which consists of a solution resistance R_s in series to the constant phase element CPE (Q) and the charge transfer resistance R_{ct} while CPE is parallel to R_{ct}. Same equivalent circuit was proposed in the literature for acidic corrosion of carbon steel in presence of quinoxaline [46]. The use of CPE-type impedance has been extensively stated by previous reports [47,48]. The impedance of CPE is described as [48,49]:

$$Z_{CPE} = A^{-1} (CE)^{-n} \quad (4)$$

where A is the CPE constant (in Ω^{-1} S^n cm^{-2}), E is the sine wave modulation angular frequency (rad^{-1}), $i^2 = -1$ is the imaginary number, and α is an empirical exponent ($0 \leq n \leq 1$), which measures the deviation from ideal capacitive behavior [50, 51].

The impedance parameters obtained by fitting the EIS data to the equivalent circuit are listed in Table 2. The inhibition efficiencies at different inhibitor concentrations were calculated by use of the equation (1).

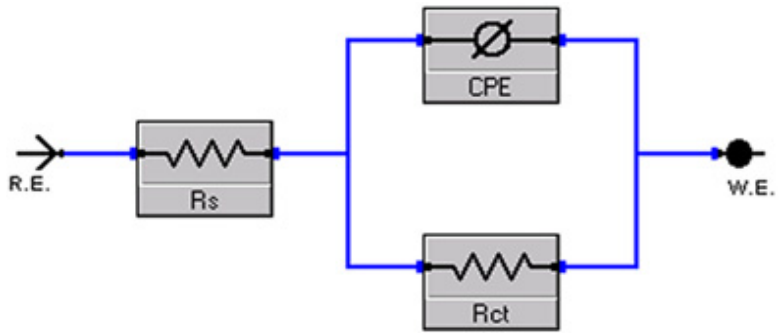

Figure 5. Electrical equivalent circuit used for modelling metal/solution interface in the absence and presence of inhibitor.

The results also show that R_{ct} values increased with increase in additive concentration. The percentage inhibition efficiencies calculated from the R_{ct} values indicate that Q3 acts as a good corrosion inhibitor for corrosion reaction of carbon steel in 1.0 HCl solution. The C_{dl} values found to decrease with increase the inhibitor concentration in the solutions. This behaviour is generally seen for system where inhibition occurred due to the formation of a surface film by the adsorption of inhibitor on the metal surface [40,52,53]. Decrease in C_{dl}, which can result from a decrease in local dielectric constant and/or an increase in the thickness of the electrical double layer, suggests that the inhibitor molecules act by adsorption at the metal/solution interface [54].

Table 2. Impedance parameters for corrosion of steel in 1.0 M HCl in the absence and presence of different concentrations of Q3 at 308 K.

Conc (M)	R_s (Ω cm^2)	R_{ct} (Ω cm^2)	n	A×10^{-4} (s^n Ω^{-1}cm^{-2})	C_{dl} (μF cm^{-2})	η_z (%)
Blank	1.67	29.66	0.91	0.146120	85.31	-----
10^{-3}	2.83	514.2	0.89	0.037286	22.87	94.2
10^{-4}	3.54	257.3	0.89	0.044422	25.56	88.5
10^{-5}	4.55	161.9	0.89	0.066920	38.25	81.7
10^{-6}	3.10	125.8	0.90	0.099004	60.82	76.4

3.3. Gravimetric study

3.3.1. Effect of concentration inhibitor

Figure 6 shows the plot of corrosion rate against inhibitor concentration for carbon steel corrosion in 1.0 M HCl at 308K from weight loss measurements. The figure reveals that the rate of corrosion of carbon steel in 1.0 M HCl decreases with increase in inhibitor concentrations at this temperature. The increase in inhibition efficiency with increase in concentration of the compound studied can be explained on the basis of increased adsorption of the compound on the metal surface. The plot of inhibition efficiency against concentration for Q3 at 308K is shown in this figure. Inspection of the figure revealed that inhibition efficiency increases with increase in the concentration of the inhibitor (Q3). Decrease in inhibition efficiency with increase in temperature may be attributed to increase in the solubility of the protective films and of any reaction products precipitated on the surface of the metal that may otherwise inhibit the reaction.

As far as the inhibition process is concerned, it is generally assumed that the adsorption of the inhibitors at the metal/aggressive solution interface is the first step in the inhibition mechanism [55]. Considering the dependence of inhibition efficiency on the concentration as represented in Figure 6, it seems to be possible that the inhibitor acts by adsorbing and blocking the available active centre for steel dissolution. In other words, the inhibitor decreases the active centre for steel dissolution. The adsorption process is made possible due to the presence of heteroatoms such as N and O which are regarded as active adsorption centres.

Q3 molecule contains nitrogen, oxygen, one phenyl ring with π electrons and quinoxaline ring. The compound could be adsorbed by the interaction between the lone pair of electrons of the oxygen and nitrogen atoms or the electron rich π systems of the aromatic rings and the quinoxaline ring and the carbon steel surface. This process as earlier reported by Umoren and Ebenso [56] may be facilitated by the presence of vacant d-orbital of iron making the steel, as observed in d-group metals or transition element. In addition to the molecular form, Q3 can be present in protonated species in an acidic solution. The formation of positively charged protonated species facilitates adsorption of the compound on the metal surface through electrostatic interaction between the organic molecules and the metal surface [57].

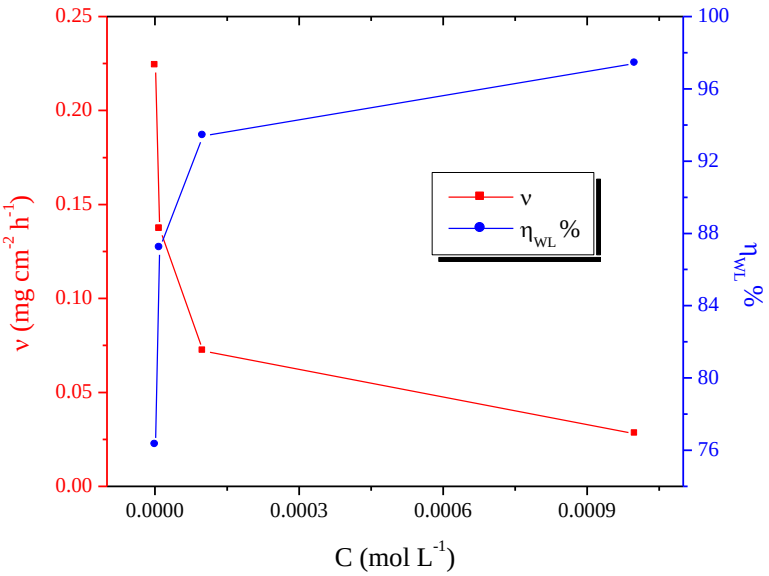

Figure 6. Variation of the corrosion rate and inhibitive efficiency against the Q3 concentrations.

3.3.2. Adsorption considerations

The interaction between the inhibitors and the steel surface can be described by the adsorption isotherm. During corrosion inhibition of metals, the nature of the inhibitor on the corroding surface has been deduced in terms of adsorption characteristics of the inhibitor. Futhermore, the solvent (H_2O) molecules could also be adsorbed at metal/solution interface. So the adsorption of organic inhibitor molecules from aqueous solution can be regarded as a quasi-substitution process between the organic compounds in the aqueous phase [$Org_{(sol)}$] and water molecules at the electrode surface [$H_2O_{(ads)}$] [58]:

$$Org_{(sol)} + xH_2O_{(ads)} \leftrightarrow xH_2O_{(sol)} + Org_{(ads)} \quad (5)$$

where x is the size ratio, that is, the number of water molecules replaced by one organic inhibitor. Basic information on the interaction between the inhibitor and the carbon steel surface can be provided by the adsorption isotherm. In order to obtain the isotherm, the linear relation between the degree of surface coverage ($\theta = \eta_{WL}\%/100$) and inhibitor concentration (C_{inh}) must be found. Attempts were made to fit the θ values to various isotherms including Langmuir, Temkin, Frumkin and Flory-Huggins. By far the best fit was obtained with the Langmuir isotherm. The Langmuir isotherm is based on the assumption that all adsorption sites are equivalent and that particle binding occurs independently from nearby sites, whether occupied or not [59]. According to this isotherm, θ is related to C_{inh} by:

$$\frac{\theta}{1-\theta} = K_{ads} C_{inh} \quad (6)$$

By rearranging this equation:

$$\frac{C_{inh}}{\theta} = \frac{1}{K_{ads}} + C_{inh} \quad (7)$$

where K_{ads} is the adsorption constant, C_{inh} is the concentration of the inhibitor and surface coverage values (θ) are obtained from the weight loss measurements for various concentrations.

Fig. 7 shows the plots of C_{inh}/θ against inhibitor concentration C_{inh} at 308K and the expected linear relationship is obtained for this compound with excellent correlation coefficent (R^2) (Table 3), confirming the validity of this approach. The slope of the straight line is unity, suggesting that adsorbed inhibitor molecules form monolayer on the carbon steel surface and there is no interaction among the adsorbed inhibitor molecules.

Table 4. Some parameters from Langmuir model for carbon steel in 1.0 M HCl at 308K.

Inhibitor	Slope	K_{ads} (M^{-1})	R^2	ΔG°_{ads} (kJ/mol)
Q3	1.02	515910.68	0.99999	-43.97

On the other hand, it was found that the kinetic thermodynamic model [60] is valid to operate the present adsorption data. The following equation represents the model [61]:

$$Ln\left(\frac{\theta}{1-\theta}\right) = LnK + yLn(C_{inh}) \quad (8)$$

The equilibrium constant of adsorption $K_{ads} = K^{(1/y)}$, where 1/y is the number of the surface active sites occupied by one inhibitor molecule and C_{inh} is the bulk concentration of the inhibitor. Values of 1/y less than unity imply the formation of multilayers of the inhibitor on the surface of the metal.

However, values of 1/y greater than unity indicate that a given inhibitor will occupy more than one active site. The plot of $Ln\left(\frac{\theta}{1-\theta}\right)$ versus Ln C_{inh} at 308 K (Fig. 3), gives straight lines with good correlation coefficients (R^2) suggesting the validity of this model for the present study. It is worth nothing that the value of 1/y is more than unity which means that the inhibitor molecule will occupy more than one active site displacing about three water molecules in the case of Q3 (Table 5).

Table 5. Some parameters from kinetic thermodynamic model for carbon steel in 1.0 M HCl at 308K.

Inhibitor	1/y	K_{ads} (M^{-1})	R^2	ΔG°_{ads} (kJ/mol)
Q3	2.84	18773555.05	0.99999	-53.17

The value of K_{ads} obtained from the Langmuir and the kinetic thermodynamic models are listed in Tables 4 and 5 respectively, together with the values of the Gibbs free energy of adsorption (ΔG°_{ads}) calculated from the equation [62]:

$$\Delta G^{\circ}_{ads} = -RTLn(55.5K_{ads}) \quad (9)$$

where R is gas constant and T is absolute temperature of experiment and the constant value of 55.5 is the concentration of water in solution in mol L^{-1}.

The high value of K_{ads} for studied quinoxaline derivative indicate stronger adsorption on the carbon steel surface in 1.0 M HCl solution. This can be explained by the presence of heteroatoms and π electrons in the inhibitor molecules. Large value of K_{ads} imply more efficient adsorption hence better inhibition efficiency [63]. The large value of K_{ads} obtained for the quinoxaline derivative agree with the high inhibition efficiency obtained.

The negative values of ΔG°_{ads} calculated from Eq. (9), are consistent with the spontaneity of the adsorption process and the stability of the adsorbed layer on the carbon steel surface. Generally, values of ΔG°_{ads} up to -20 kJ mol^{-1} are consistent with physisorption, while those around -40 kJ mol^{-1} or higher are associated with chemisorption as a result of the sharing or transfer of electrons from organic molecules to the metal surface to form a coordinate bond [64]. In the present study, the calculated standard free energy of adsorption value is closer to -40 kJ mol^{-1} (Tables 4 and 5). Therefore it can be concluded that the adsorption of the Q3 on the carbon steel surface is more chemical than physical one. [65].

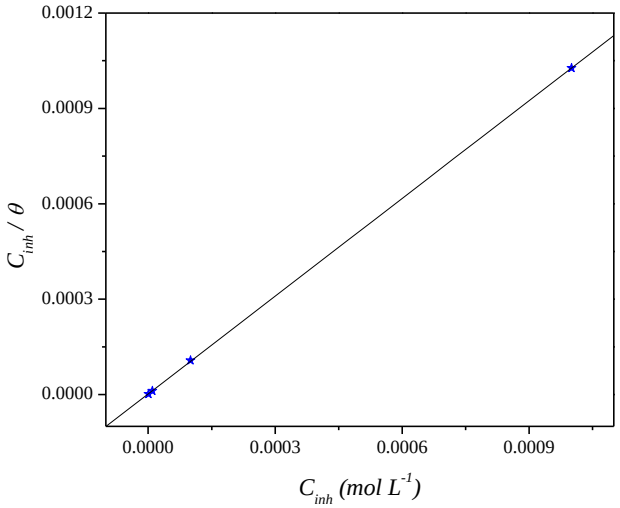

Figure 7. Langmuir adsorption of Q3 on the carbon steel surface in 1.0 HCl solution.

3.4. Quantum chemical calculations

Recently, quantum chemical calculations have proved to be a very powerful tool for studying corrosion inhibition mechanisms [66].

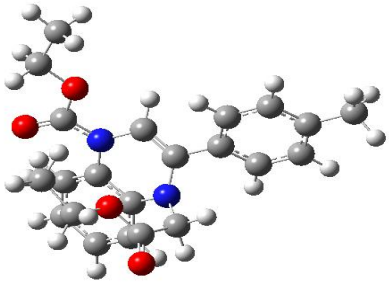

Figure 7. Optimized structure of studied molecule obtained by B3LYP/6-31G* level.

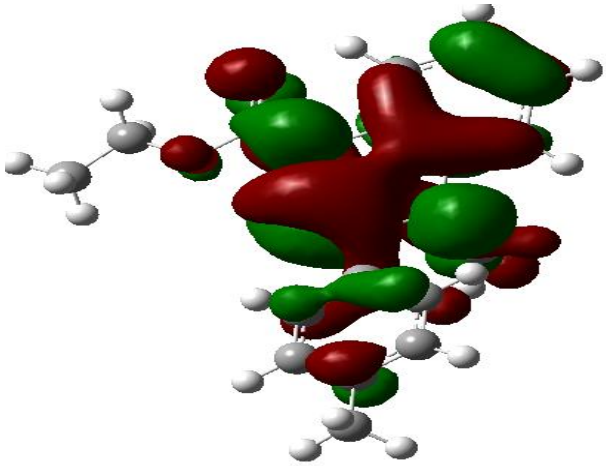

HOMO

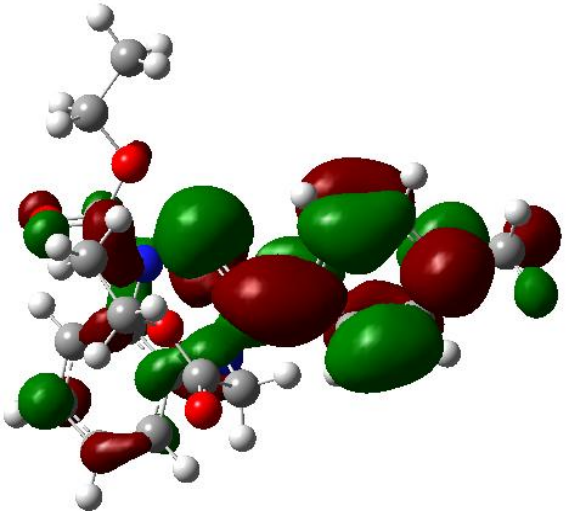

LUMO

Figure 8. Schematic representation of HOMO and LUMO molecular orbital of studied molecules.

Theoretical prediction of the efficiency of corrosion inhibitors has become very popular in parallel with the progress in computational hardware and the development of efficient algorithms which assisted the routine development of molecular quantum mechanical calculations [67]. All

quantum chemical properties were obtained after geometric optimization with respect to the all nuclear coordinates using Kohn-Sham approach at DFT level. The optimized structure of the studied compound as shown in Fig. 7. In Fig. 8, we have presented **t**he frontier molecule orbital density distributions of the studied compound. Analysis of Fig. 3 shows that the distribution of two energies HOMO and LUMO, we can see that the electron density of the HOMO and LUMO location was distributed almost of the entire molecule.

Table 6. Calculated quantum chemical parameters of the studied compound.

Quantum parameters	Q3
E_{HOMO} (eV)	-4.8066
E_{LUMO} (eV)	-0.695
ΔE gap (eV)	4.1716
μ (debye)	3.0849
$I = -E_{HOMO}$ (eV)	4.8066
$A = -E_{LUMO}$ (eV)	0.695
$\chi = \frac{I + A}{2}$ (eV)	2.7508
$\eta = \frac{I - A}{2}$ (eV)	2.0558
$\sigma = \frac{1}{\eta}$	0.48643
$\Delta N = \frac{\chi_{Fe} - \chi_{inh}}{2(\eta_{Fe} + \eta_{inh})}$	1.0334663
TE (eV)	-1263.220327

The total energy for our studied molecule calculated by DFT quantum chemical methods is equal to-1263.220327 eV. Hohenberg and Kohn [68] proved that the total energy of a system including that of the many body effects of electrons (exchange and correlation) in the presence of static external potential (for example, the atomic nuclei) is a unique functional of the charge density. The minimum value of the total energy functional is the ground state energy of the system. The electronic charge density which yields this minimum is then the exact single particle ground state energy. On the other hand, the transition of electron, according to the frontier molecular orbital theory of chemical reactivity, is due to interaction between highest occupied molecular orbital (HOMO) and lowest unoccupied molecular orbital (LUMO) of reacting species. E_{HOMO} is a quantum chemical parameter which is often associated with the electron donating ability of the molecule. High value of E_{HOMO} is likely to a tendency of the molecule to donate electrons to appropriate acceptor molecule of low empty molecular orbital energy [69]. The inhibitor does not only donate electron to the unoccupied d orbital

of the metal ion but can also accept electron from the d-orbital of the metal leading to the formation of a feed back bond. The highest value of E_{HOMO} -4.8066 eV of the studied compound indicates the better inhibition efficiency. On the other hand, It has also been found that an inhibitor does not only donate an electron to the unoccupied d orbital of the metal ion but can also accept electrons from the d orbital of the metal leading to the formation of a feedback bond. Therefore, the tendency for the formation of a feedback bond would depend on the value of E_{LUMO}. The obtained value of the E_{LUMO} = -0.695 eV indicates the easier of the acceptance of electrons from the d orbital of the metal [70,71]. The band gap energy, $\Delta E = E_{LUMO} - E_{HOMO}$ is an important parameter as a function of reactivity of the inhibitor molecule towards the adsorption on metallic surface. As ΔE decreases, the reactivity of the molecule increases leading to increase the inhibition efficiency of the molecule. The calculations indicate that our studied molecule has a small value of gap energy (4.171 eV) which means the highest reactivity and accordingly the highest inhibition efficiency which agrees well with the experimental observations. Absolute hardness and softness are important properties to measure the molecular stability and reactivity. It is apparent that the chemical hardness fundamentally signifies the resistance towards the deformation or polarization of the electron cloud of the atoms, ions or molecules under small perturbation of chemical reaction. A hard molecule has a large energy gap and a soft molecule has a small energy gap [72]. In our present work the studied molecule has low hardness value 2.055 eV and a highest value of softness of 0.486. Finally and in order to describe the global polarity of a polar covalent bond the studied compound, we have determined from the optimization structure the total dipole moment. For a complete molecule the total molecular dipole moment may be approximated as the vector sum of individual bond dipole moments. The dipole moment (μ in Debye) is another important electronic parameter that results from non uniform distribution of charges on the various atoms in the molecule. The high value of dipole moment probably increases the adsorption between chemical compound and metal surface [73, 74]. In our study, the value of the dipole moment is 3.084 debye.

4. CONCLUSION

In this study, it was shown that ethyl 2-(4-(2-ethoxy-2-oxoethyl)-2-*p*-tolylquinoxalin-1(4*H*)-yl) acetate (Q3), is effective inhibitor of corrosion of carbon steel exposed to 1.0 M HCl. In determining the corrosion rate, electrochemical studies and weight loss measurements give comparable results. Polarisation studies showed that inhibitor was mixed-type inhibitor in 1.0 M HCl and its inhibition efficiency increased with the inhibitor concentration. Data obtained from ac impedance technique show a frequency distribution and therefore a modelling element with frequency dispersion behaviour, a constant phase element (CPE) has been used. The analysis of degree of surface coverage of this compound showed the linearity of Langmuir isotherm adsorptions, which represent the monolayer formation of this compound on carbon steel surface. The free Gibbs adsorption energy values, ΔG°_{ads}, of synthesized compound is negative, which indicated the spontaneity of adsorption process of this compound on carbon steel surface. The correlation between the quantum chemical parameters and inhibition efficiency was investigated using DFT/B3LYP calculations. The inhibition efficiency of the inhibitor are closely related to the quantum chemical parameters, the highest occupied molecular

orbital (E_{HOMO}), energy of lowest unoccupied molecular orbital (E_{LUMO}), HOMO–LUMO energy gap (ΔE_{H-L}), the hardness (σ), the softness (η), the dipole moment (μ) and the total energy (TE).

ACKNOWLEDGEMENTS
Prof S. S. Al-Deyab and Prof B. Hammouti extend their appreciation to the Deanship of Scientific Research at king Saud University for funding the work through the research group project.

References

1. G. Schmitt, *Br. Corros. J.* 19 (1984) 165.
2. D.D.N. Singh, T.B. Singh, B. Gaur, *Corros. Sci*. 37 (1995) 1005.
3. P. Morales-Gil, G. Negrón-Silva, M. Romero-Romo, C. Ángeles-Chávez, M. Palomar-Pardavé, *Electrochim. Acta* 49 (2004) 4733.
4. M. Bouklah, A. Ouassini, B. Hammouti, A. El Idrissi, *Appl. surf. Sci.* 250 (2005) 50.
5. Mayuri N. Katariya, Arun K. Jana, Parimal A. Parikh, *J. Ind. Eng. Chem.* 19 (2013) 286.
6. H. Zarrok, H. Oudda, A. Zarrouk, R. Salghi, B. Hammouti, M. Bouachrine , *Der Pharm. Chem*. 3 (2011) 576.
7. H. Zarrok, R. Salghi, A. Zarrouk, B. Hammouti, H. Oudda, Lh. Bazzi, L. Bammou, S. S. Al-Deyab, *Der Pharm. Chem*. 4 (2012) 407.
8. L. Wang, *Corros. Sci*, 43 (2001) 2281.
9. A. Popova, M. Christov, T. Deligeorgiev, *Corrosion*, 59 (2003) 756.
10. K. F. Khaled, *Electrochim. Acta*, 48 (2003) 2493.
11. F. Zhang, Y. Tang, Z. Cao, W. Jing, Z. Wu, Y. Chen, *Corros. Sci, 61 (2012) 1.*
12. I. B. Obot, N.O. Obi-Egbedi, *Corros. Sci*, 52 (2010) 657.
13. I. Ahamad, M.A. Quraishi, *Corros. Sci*, 51 (2009) 2006.
14. A. Popova, M. Christov, A. Vasilev, *Corros. Sci*, 49 (2007) 3290.
15. A. Zarrouk, M. Messali, M. R. Aouad, M. Assouag, H. Zarrok, R. Salghi, B. Hammouti, A. Chetouani, *J. Chem. Pharm. Res*. 4 (2012) 3427.
16. D. Ben Hmamou, M. R. Aouad, R. Salghi, A. Zarrouk, M. Assouag, O. Benali, M. Messali, H. Zarrok, B. Hammouti, *J. Chem. Pharm. Res*. 4 (2012) 3489.
17. H. Zarrok, H. Oudda, A. El Midaoui, A. Zarrouk, B. Hammouti, M. Ebn Touhami, A. Attayibat,S. Radi, R. Touzani, *Res. Chem. Intermed* (2012) DOI 10.1007/s11164-012-0525-x
18. A. Zarrouk, B. Hammouti, H. Zarrok, R. Salghi, A. Dafali, Lh. Bazzi, L. Bammou, S. S. Al-Deyab, *Der Pharm. Chem*. 4 (2012) 337.
19. M. Christov, A. Popova, *Corros. Sci*, 46 (2004) 1613.
20. F. Bentiss, M. Traisnel, H. Vezin, M. Lagrenée, *Corros. Sci, 45 (2003)371.*
21. E.A. Noor, A.H. Al-Moubaraki, *Corros. Sci*, 51 (2009) 868
22. M. Outirite, M. Lagrenée, M. Lebrini, M. Traisnel, C. Jama, H. Vezin, F. Bentiss, *Electrochim. Acta*, 55 (2010) 1670.
23. M.M. Ibrahim, M.A. Amin, K. Ichikawa, *J. Mol. Struct*, 985 (2011) 191.
24. K.C. Emregül, M. Hayvalı, *Mater. Chem. Phys*. 83 (2004) 209.
25. H. Zarrok, A. Zarrouk, B. Hammouti, R. Salghi, C. Jama, F. Bentiss, *Corros. Sci*. 64 (2012) 243.
26. A.D. Becke. *J. Chem. Phys*. 96 (1992) 9489.
27. A.D. Becke. *J. Chem. Phys*. 98 (1993) 1372.
28. C. Lee, W. Yang, R.G. Parr. *Phys. Rev. B.* 37 (1988) 785.
29. Gaussian 03, Revision B.01, M. J. Frisch, et al., Gaussian, Inc., Pittsburgh, PA, (2003).
30. H. Ashassi-Sorkhabi, B. Shaabani, D. Seifzadeh, *Appl. Surf. Sci*. 239 (2005) 154.
31. R. Fletcher, Practical Methods of Optimization, vol. 1, Wiley, New York, (1980).

32. L. Afia, R. Salghi, E. Bazzi, A. Zarrouk, B. Hammouti, M. Bouri, H. Zarrouk, L. Bazzi, L. Bammou, *Res. Chem. Intermed* (2012) doi: 10.1007/s11164-012-0496-y.
33. H. Zarrok, A. Zarrouk, R. Salghi, B. Hammouti, M. Elbakri, M. Ebn Touhami, F. Bentiss, H. Oudda, *Res. Chem. Intermed* (2013) doi: 10.1007/s11164-012-1004-0.
34. S. Belkaid, K. Tebbji, A. Mansri, A. Chetouani, B. Hammouti, *Res. Chem. Interm*. 38 (2012) 2309.
35. K.F. Khaled, *Appl. surf. Sci*. 252 (2006) 4120.
36. G. Avci, *Coll. Surf. PhysicoChem. Eng. Asp*. 317 (2008) 730.
37. M. M. Saleh, A. A. Atia, *J. Appl. Electrochem.* 36 (2006) 899.
38. D. Ben Hmamou, R. Salghi, A. Zarrouk, B. Hammouti, O. Benali, H. Zarrok, S. S. Al-Deyab, *Res. Chem. Intermed* (2012) doi: 10.1007/s11164-012-0892-3.
39. M. Larif, A. Elmidaoui, A. Zarrouk, H. Zarrok, R. Salghi, B. Hammouti, H. Oudda, F. Bentiss, *Res. Chem. Intermed* (2012) doi: 10.1007/s11164-012-0892-3.
40. M. Behpour, S.M. Ghoreishi, N. Soltani, M. Salavati-Niasari, *Corros. Sci*. 51 (2009) 1073.
41. R. Solmaz, *Corros. Sci*. 52 (2010) 3321.
42. M. Benabdellah, R. Touzani, A. Aouniti, A. Dafali, S. Elkadiri, B. Hammouti, M. Benkaddour, *Phys. Chem. News*. 37 (2007) 63.
43. M. Elayyachy, B. Hammouti, A. El Idrissi and A. Aouniti, *Port. Electrochim. Acta*. 29 (2011) 57.
44. K. Adardour, R. Touir, Y. Ramli, R. A. Belakhmima, M. Ebn Touhami, C. Kalonji Mubengayi, H. El Kafsaoui, E. M. Essassi, *Res. Chem. Intermed* (2012) doi: 10.1007/s11164-012-0719-2.
45. H. Zarrok, A. Zarrouk, R. Salghi, Y. Ramli, B. Hammouti, M. Assouag, E. M. Essassi, H. Oudda, and M. Taleb, *J. Chem. Pharm. Res*. 12 (2012) 5048.
46. F. Bentiss, C. Jama, B. Mernari, H. El Attari, L. El Kadi, M. Lebrini, M. Traisnel, M. Lagrenee, *Corros. Sci.* 51 (2009) 1628.
47. A. Popova, M. Christov, *Corros. Sci*. 48 (2006) 3208.
48. K.S. Jacob, G. Parameswaran, *Corros. Sci*. 52 (2010) 224.
49. I. Ahamad, R. Prasad, M.A. Quraishi, *Mater. Chem. Phys*. 124 (2010) 1155.
50. E.S. Ferreira, C. Giancomlli, F.C. Giacomlli, A. Spinelli, *Mater. Chem. Phys*. 83 (2004) 129
51. L.J.M. Vracˇar, D.M. Drazˇic, *Corros. Sci*. 44 (2002) 16.
52. N.A. Negm, F.M. Ghuiba, S.M. Tawfik, *Corros. Sci*. 53 (2011) 3566.
53. D.P. Schweinsberg, G.A. George, A.K. Nanayakkara, D.A. Steiner, *Corros. Sci.* 28 (1988) 33.
54. G. Bereket, A. Yurt, *Corros. Sci*. 43 (2001) 1179.
55. L. Niu, H. Zhang, F. Wei, S. Wu, X. Cao, P. Lui., *Appl. Surf. Sci*., 252 (2005) 1634.
56. S.A.Umoren and E.E.Ebenso, *Mater. Chem. Phys*. 106 (2007) 387.
57. Y. Feng, K.S. Siow, W. K. Teo, A.K. Hsieh. *Corros. Sci*. 41 (1999) 829.
58. M. Sahin, S. Bilgic, H. Yilmaz, *Appl. Surf. Sci.* 195 (2002) 1.
59. G. Avci, *Colloids and Surfaces A: Physicochem.Eng. Aspects*. 317 (2008) 736.
60. G.Y. Elewady, H.A. Mostafa, *Desalination* 247 (2009) 573.
61. D.W. Atkins, Physical Chemistry, Oxford University Press, Oxford, 5th ed., p. 992 (1994).
62. R. Solmaz, G. Kardas, M. Culha, B. Yazici, M. Erbil, *Electrochim. Acta*. 53 (2008) 5941.
63. S.A. Refay, F. Taha, A.M. Abd El-Malak, *Appl. Surf. Sci.* 236 (2004) 175.
64. G. Moretti, F. Guidi, G. Grion, *Corros. Sci.* 46 (2004) 387.
65. K. Mallaiyaa, R. Subramaniama, S.S. Srikandana, S. Gowria, N. Rajasekaranb, A. Selvaraj, *Electrochim. Acta*, 56 (2011) 3857.
66. F. B. Growcock, *Corrosion*. 45 (1989) 1003.
67. A. Domenicano, I. Hargittai, Accurate Molecular Structures, Their Determination and Importance, Oxford University Press, New York, (1992).
68. H. Ju, Z.P. Kai, Y. Li, *Corros. Sci*. 50 (2008) 865.
69. M. J. S. Dewar, W. Thiel, *J. Am. Chem. Soc*., 99 (1977) 4899.

70. A.Y. Musa, A. H. Kadhum, A. B. Mohamad, A.b. Rohoma, H. Mesmari, *J. Mol. Struct*. 969 (2010) 233.
71. M.A. Amin, K.F. Khaled, S.A. Fadl-Allah, *Corros. Sci*., 52 (2010) 140.
72. G. Gece, S. Bilgic, *Corros. Sci*. 51 (2009) 1876.
73. E.E. Ebenso, D.A. Isabirye, N.O. Eddy, *Int. J. Mol. Sci*. 11 (2010) 2473.
74. O. Kikuchi, *Quant. Struct.-Act. Relat*. 6 (1987) 179.